822 *Organometallics* **1994,** *13,* 822–829

Reactivity of Bis(alkyne) Carborane Complexes of Molybdenum and Tungsten toward *tert*-Butyl Isocyanide[†]

Stephen J. Dossett, Sihai Li, Donald F. Mullica, Eric L. Sappenfield, and F. Gordon A. Stone*

Department of Chemistry, Baylor University, Waco, Texas 76798-7348

Received September 16, 1993[⊗]

Treatment of the complex [Mo(CO)(η^2-MeC$_2$Me)$_2$(η^5-7,8-Me$_2$-7,8-C$_2$B$_9$H$_9$)] (**5a**) in CH$_2$Cl$_2$ with ca. 4 mol equiv of CNBu^t affords the compounds [Mo(CO)(CNBu^t)$_3$(η^5-7,8-Me$_2$-7,8-C$_2$B$_9$H$_9$)] (**6**) and [Mo(CNBu^t)$_4$(η^5-7,8-Me$_2$-7,8-C$_2$B$_9$H$_9$)] (**7a**). However, reactions between [M(CO)(η^2-MeC$_2$Me)$_2$(η^5-7,8-C$_2$B$_9$H$_{11}$)] (**5b**, M = Mo; **5c**, M = W) and an excess of CNBu^t in CH$_2$Cl$_2$ give [M(CNBu^t)$_4$(η^5-7,8-C$_2$B$_9$H$_{11}$)] (**7b**, M = Mo; **7c**, M = W) and [M{=C[N(H)Bu^t]C(Me)=C(Me)[C(O)N(H)Bu^t]}(CNBu^t)$_2$(η^5-7,8-C$_2$B$_9$H$_{11}$)] (**8a**, M = Mo; **8b**, M = W). The structure of **8b** has been established by an X-ray diffraction study. Crystals are triclinic, space group $P\bar{1}$ (No. 2) with a = 10.913(2) Å, b = 11.992(2) Å, c = 14.852(2) Å, α = 73.12(1)°, β = 82.48(1)°, γ = 74.138(16)°, and Z = 2. The tungsten atom is ligated by the *nido*-C$_2$B$_9$H$_{11}$ cage in the normal pentahapto manner, by two isocyanide molecules (W–CNBu^t average 2.02 Å), and by a vinylcarbene moiety [W=C = 2.018(7) Å, W–C = 2.308(8) and 2.335(8) Å]. The latter group is formed at the metal center by coupling of one but-2-yne ligand with two isocyanide molecules, followed by reaction with H$_2$O. Methylation of the complex [Mo(CNBu^t)$_4$(η^5-7,8-C$_2$B$_9$H$_{11}$)] (**7b**) with CF$_3$SO$_3$Me yields initially the species [MoMe(CNBu^t)$_4$(η^5-7,8-C$_2$B$_9$H$_{11}$)][SO$_3$CF$_3$] (**9**), which rearranges to [Mo(CNBu^t)$_3${η^2-C(Me)=NBu^t}(η^5-7,8-C$_2$B$_9$H$_{11}$)][SO$_3$CF$_3$] (**10**). The structure of **10** has been determined by X-ray diffraction. Crystals are monoclinic, space group $C2/c$ (No. 15) with a = 41.569(4) Å, b = 9.465(2) Å, c = 20.381(2) Å, β = 105.616(7)°, and Z = 8. The molybdenum atom is coordinated by a *nido*-C$_2$B$_9$H$_{11}$ cage, three isocyanide molecules (Mo–CNBu^t average 2.11 Å), and an η^2-C(Me)=NBu^t moiety [Mo–C = 2.10(1) Å, Mo–N = 2.14(1) Å]. In addition to the X-ray crystal structure determinations, the IR and NMR data for the new complexes are reported and discussed in relation to their structures.

Introduction

We have recently reported the synthesis of several bis(alkyne) carborane complexes of molybdenum and tungsten.[1,2] Some interesting reactivity patterns of these species have been observed. For example, under certain circumstances the coordinated alkyne molecules may couple with the carborane cage at a molybdenum center.[1b] Thus in CH$_2$Cl$_2$, the complex [Mo(CO)(PPh$_3$)(η^2-PhC$_2$Ph)(η^5-7,8-Me$_2$-7,8-C$_2$B$_9$H$_9$)] (**1**) (Chart 1) yields a mixture of [Mo(CO)$_3$(PPh$_3$)(η^5-7,8-Me$_2$-7,8-C$_2$B$_9$H$_9$)] and [Mo(CO)$_2$(PPh$_3$){η^2,η^5-7,8-Me$_2$-10-[C(Ph)=C(H)Ph]-7,8-C$_2$B$_9$H$_8$}] (**2**). The latter species is formed via an insertion process between the coordinated PhC$\equiv$CPh and a B–H bond of the carborane cage. If a CH$_2$Cl$_2$ solution of the complex [Mo(CO)(η^2-HC$_2$SiMe$_3$)$_2$(η^5-7,8-Me$_2$-7,8-C$_2$B$_9$H$_9$)] (**3a**) is stirred for several hours at room temperature, the species [Mo(CO)(η^2-HC$_2$SiMe$_3$){η^2,η^5-7,8-Me$_2$-10-[C(H)=C(H)SiMe$_3$]-7,8-C$_2$B$_9$H$_8$}] (**4a**) is obtained. Moreover, synthesis of the deuteriated compound **4b** from **3b**, the latter generated *in situ* from [N(PPh$_3$)$_2$][Mo(CO)$_2$(η^3-C$_3$H$_5$)(η^5-7,8-Me$_2$-7,8-C$_2$B$_9$H$_9$)], Me$_3$SiC$\equiv$CD, and HBF$_4$·Et$_2$O, revealed from NMR studies that insertion of the alkyne into the cage B–H bond proceeds via the intermediacy of a molybdenum–vinylidene species.

Chart 1

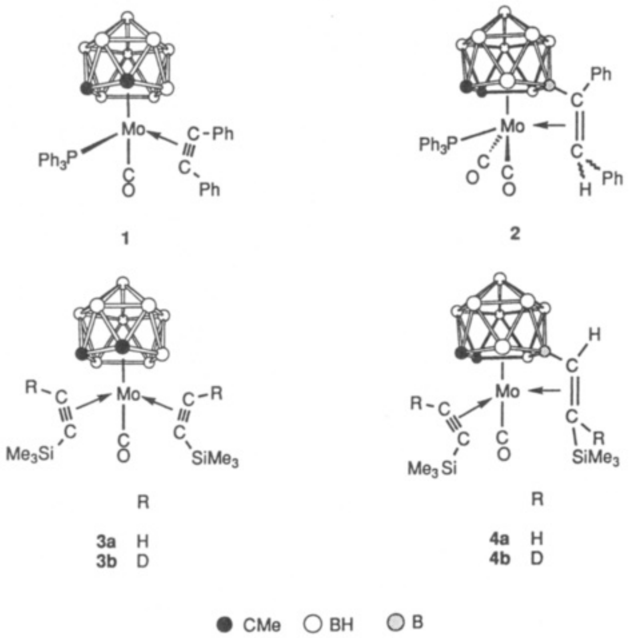

1

2

	R
3a	H
3b	D

	R
4a	H
4b	D

We have also reported reactions between bis(alkyne) carborane complexes of molybdenum and tungsten and the tertiary phosphines PMe$_3$, PMe$_2$Ph, and PPh$_3$.[1,2a] Simple substitution of one of the ligated alkyne groups

---

[*] To whom correspondence should be addressed.

[†] In this paper Mo or W atoms form with [*nido*-7,8-R'$_2$-7,8-C$_2$B$_9$H$_9$]$^{2-}$ anions *closo*-1,2-dicarba-3-metalladodecaborane structures. However, in the formulas the carborane group is designated as η^5-7,8-R'$_2$-7,8-C$_2$B$_9$H$_9$ in order to emphasize its pentahapto ligand character in which it formally acts as a four-electron donor, related to the five-electron donor η^5-C$_5$H$_5$.

[⊗] Abstract published in *Advance ACS Abstracts,* January 15, 1994.

(1) (a) Dossett, S. J.; Li, S.; Stone, F. G. A. *J. Chem. Soc., Dalton Trans.* **1993**, 1585. (b) Dossett, S. J.; Li, S.; Mullica, D. F.; Sappenfield, E. L.; Stone, F. G. A. *J. Chem. Soc., Dalton Trans.* **1993**, 3551.

(2) (a) Brew, S. A.; Devore, D. D.; Jenkins, P. D.; Pilotti, M. U.; Stone, F. G. A. *J. Chem. Soc., Dalton Trans.* **1992**, 393. (b) Jeffery, J. C.; Li, S.; Sams, D. W. I.; Stone, F. G. A. *J. Chem. Soc., Dalton Trans.* **1992**, 877. (c) Jeffery, J. C.; Li, S.; Stone, F. G. A. *Organometallics* **1992**, *11*, 1902.

0276-7333/94/2313-0822$04.50/0

Table 1. Physical and Infrared Absorption Data

no.	compd	color	yield/%	$\nu_{max}(NC)^a$/cm^{-1}	anal.^{b}/% C	H	N
5c	$[W(CO)(\eta^2\text{-}MeC_2Me)_2(\eta^5\text{-}7,8\text{-}C_2B_9H_{11})]$	pale yellow	63	*2044 vs	30.1 (29.2)	5.7 (5.1)	
6	$[Mo(CO)(CNBu^t)_3(\eta^5\text{-}7,8\text{-}Me_2\text{-}7,8\text{-}C_2B_9H_9)]$	yellow	30	2160 s, 2119 vs, *1980 s	44.9 (45.0)	8.0 (7.9)	7.8 (7.9)
7a	$[Mo(CNBu^t)_4(\eta^5\text{-}7,8\text{-}Me_2\text{-}7,8\text{-}C_2B_9H_9)]$	yellow	43	2139 s, 2092 vs, 2051 vs	47.9 (49.0)	9.5 (8.7)	9.1 (9.5)
7b	$[Mo(CNBu^t)_4(\eta^5\text{-}7,8\text{-}C_2B_9H_{11})]$	yellow	61	2144 m, 2084 vs, 2047 vs	46.5 (47.1)	9.0 (8.5)	9.7 (10.0)
7c	$[W(CNBu^t)_4(\eta^5\text{-}7,8\text{-}C_2B_9H_{11})]$	yellow	36	2139 m, 2083 sh, 2035 vs	41.6 (40.7)	7.4 (7.3)	8.3 (8.6)
8a	$[Mo\{=C[N(H)Bu^t]C(Me)=C(Me)[C(O)N(H)Bu^t]\}\text{-}(CNBu^t)_2(\eta^5\text{-}7,8\text{-}C_2B_9H_{11})]$	orange-red	11	2134 s, 2112 sh, 2071 sh^c	50.1 (49.3)	8.7 (8.8)	8.8 (8.9)
8b	$[W\{=C[N(H)Bu^t]C(Me)=C(Me)[C(O)N(H)Bu^t]\}\text{-}(CNBu^t)_2(\eta^5\text{-}7,8\text{-}C_2B_9H_{11})]$	orange-red	38	2127 s, 2104 sh, 2066 sh^d	43.0 (43.3)	7.8 (7.7)	7.5 (7.8)
9	$[MoMe(CNBu^t)_4(\eta^5\text{-}7,8\text{-}C_2B_9H_{11})][SO_3CF_3]$	orange	69	2211 m, 2183 vs, 2150 sh	39.9 (39.8)	6.9 (7.0)	7.6 (7.7)
10	$[Mo(CNBu^t)_3\{\eta^2\text{-}C(Me)=NBu^t\}(\eta^5\text{-}7,8\text{-}C_2B_9H_{11})]\text{-}[SO_3CF_3]$	orange	60	2197 s, 2171 vs, 1756 w	39.9 (39.8)	6.9 (7.0)	7.6 (7.7)

[a] Measured in CH_2Cl_2. For all carborane compounds there is a broad band at ca. 2550 cm^{-1} due to B–H absorptions. Peaks due to $\nu_{max}(CO)$ are labeled with an asterisk. [b] Calculated values are given in parentheses. [c] Weak bands measured at 1622 and 1586 cm^{-1} are due to $\nu_{max}(NC)$ and $\nu_{max}(CO)$ of the vinylcarbene group. [d] Weak absorptions at 1625 and 1580 cm^{-1} are due to $\nu_{max}(NC)$ and $\nu_{max}(CO)$ bands of the vinylcarbene group.

Chart 2

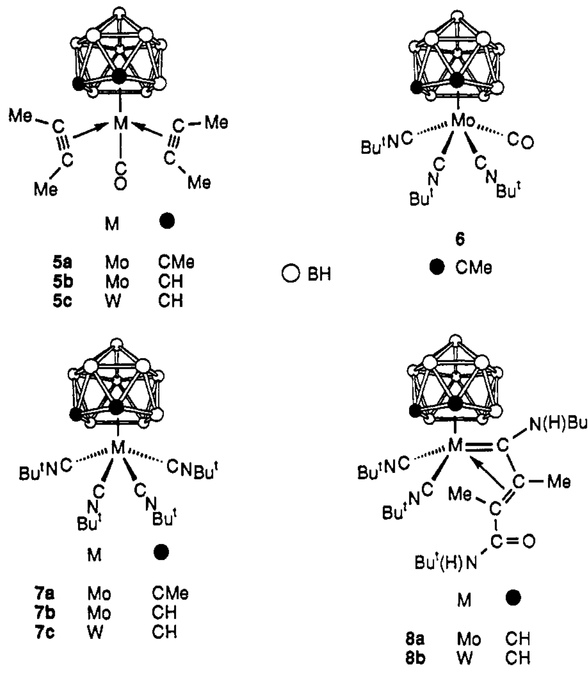

with the phosphine was observed. For example, complex **1** was isolated in good yield from the reaction of the compound $[Mo(CO)(\eta^2\text{-}PhC_2Ph)_2(\eta^5\text{-}7,8\text{-}Me_2\text{-}7,8\text{-}C_2B_9H_9)]$ with PPh_3.

In this paper, we report studies on the reactivity of the complexes $[M(CO)(\eta^2\text{-}MeC_2Me)_2(\eta^5\text{-}7,8\text{-}R'_2\text{-}7,8\text{-}C_2B_9H_9)]$ (**5a**, M = Mo, R′ = Me; **5b**, M = Mo, R′ = H; **5c**, M = W, R′ = H) toward *tert*-butyl isocyanide. It was hoped that the isocyanide complexes formed would be easily methylated by CF_3SO_3Me to give cationic salts of carborane metal species, the chemistry of which is as yet uninvestigated.

Results and Discussion

The compounds **5a,b** (Chart 2) have been previously prepared.[1a] For the present study the new compound **5c** was synthesized by protonation of the salt $[N(PPh_3)_2][W(CO)_2(\eta^3\text{-}C_3H_5)(\eta^5\text{-}7,8\text{-}C_2B_9H_{11})]$ with $HBF_4\cdot Et_2O$ in the presence of but-2-yne in excess. Complex **5c** was fully characterized by the data given in Tables 1–3. As expected, the spectroscopic properties are similar to those of **5a,b**.[1a]

Treatment of complex **5a** in CH_2Cl_2 with ca. 4 equiv of $CNBu^t$ gave a mixture of the tris- and tetrakis(isocyanide) species $[Mo(CO)(CNBu^t)_3(\eta^5\text{-}7,8\text{-}Me_2\text{-}7,8\text{-}C_2B_9H_9)]$ (**6**) and $[Mo(CNBu^t)_4(\eta^5\text{-}7,8\text{-}Me_2\text{-}7,8\text{-}C_2B_9H_9)]$ (**7a**), respectively, separated by column chromatography on alumina. In both products the alkyne ligands of the precursor **5a** have been displaced by $CNBu^t$. Data characterizing compounds **6** and **7a** are listed in Tables 1–3. The IR spectrum of **6** shows a CO stretching band at 1980 cm^{-1}. Two N≡C absorption frequencies are observed at 2160 and 2119 cm^{-1}, with the latter being the stronger in intensity. In the ^1H NMR spectrum there are two resonances at δ 1.52 and 1.53 ppm, arising from the two nonequivalent $CNBu^t$ environments as expected. The latter signal is double the intensity of the former and is therefore due to the two *transoid* $CNBu^t$ ligands. As expected, the two equivalent cage CMe groups give a single peak at δ 2.05 ppm. In accord with the formulation of **6**, the $^{13}C\{^1H\}$ NMR spectrum shows a single resonance at δ 246.7 ppm due to the carbonyl group. There are also two broad signals at δ 170.6 and 167.8 ppm ascribable to the *C*NBu^t nuclei. Resonances at δ 68.1 and 31.0 ppm are assigned to the cage *C*Me and C*Me* nuclei, respectively. The remaining peaks are also readily assigned (Table 2). The $^{11}B\{^1H\}$ NMR data (Table 3) for **6** are as expected.

In the ^1H NMR spectrum of **7a** only one signal is observed at δ 1.50 ppm for the four $CNBu^t$ ligands, as expected. The cage CMe groups resonate at δ 2.00 ppm. Correspondingly, the $^{13}C\{^1H\}$ NMR spectrum of **7a** shows three resonances for the $CNBu^t$ ligands at δ 185.3 (NC), 57.3 (CMe_3), and 31.3 ppm (CMe_3).

During chromatography of the reaction mixture containing complexes **6** and **7a**, trace amounts of an orange species were observed on the column. This species was not identified due to its low yield. However, the probable nature of this very minor product was revealed by a study of the reaction between CH_2Cl_2 solutions of **5b** and ca. 4 mol equiv of $CNBu^t$ at room temperature. After chromatographic separation, two compounds were isolated, a yellow species characterized as $[Mo(CNBu^t)_4(\eta^5\text{-}7,8\text{-}C_2B_9H_{11})]$ (**7b**), akin to **7a**, and the orange-red species $[Mo\{=C[N(H)Bu^t]C(Me)=C(Me)[C(O)N(H)Bu^t]\}(CNBu^t)_2(\eta^5\text{-}7,8\text{-}C_2B_9H_{11})]$ (**8a**). The reaction between **5c** and $CNBu^t$ gave the analogous tungsten complexes $[W(CNBu^t)_4(\eta^5\text{-}7,8\text{-}C_2B_9H_{11})]$ (**7c**) and $[W\{=C[N(H)Bu^t]C(Me)=C(Me)[C(O)N(H)Bu^t]\}(CNBu^t)_2(\eta^5\text{-}7,8\text{-}C_2B_9H_{11})]$ (**8b**). The spectroscopic properties of **7b,c** are similar to those of **7a** (Tables 1–3) and are not therefore discussed in detail. However, the nature of the compounds

Table 2. Hydrogen-1 and Carbon-13 NMR Data[a]

compd	^{1}H/δ[b]	^{13}C/δ[c]
5c	2.870 (s, 6 H, Me), 2.871 (s, 6 H, Me), 2.97 (s, br, 2 H, CH)	214.2 [CO, J(WC) = 124], 166.9 [$\equiv$C, J(WC) = 42], 143.6 [$\equiv$C, J(WC) = 13], 46.8 (br, CH), 16.33, 16.26 (Me)
6	1.52 (s, 9 H, Me$_3$), 1.53 (s, 18 H, Me$_3$), 2.05 (s, 6 H, Me)	246.7 (CO), 170.6 (br, 2 × NC), 167.8 (br, NC), 68.1 (br, *C*Me), 58.8 (2 × *C*Me$_3$), 58.2 (*C*Me$_3$), 31.0 (C*Me*), 30.9 (C*Me*$_3$), 30.7 (2 × C*Me*$_3$)
7a	1.50 (s, 36 H, Me$_3$), 2.00 (s, 6 H, Me)	185.3 (br, NC), 61.0 (br, *C*Me), 57.3 (*C*Me$_3$), 31.3 (C*Me*$_3$), 29.0 (C*Me*)
7b	1.50 (s, 36 H, Me$_3$), 2.51 (s, br, 2 H, CH)	182.8 (br, NC), 57.9 (*C*Me$_3$), 40.2 (br, CH), 31.3 (C*Me*$_3$)
7c	1.49 (s, 36 H, Me$_3$), 2.71 (s, br, 2 H, CH)	172.1 (br, NC), 58.4 (*C*Me$_3$), 38.0 (br, CH), 31.9 (C*Me*$_3$)
8a	1.16 (s, 9 H, Me$_3$), 1.36 (s, 9 H, Me$_3$), 1.49 (s, 9 H, Me$_3$), 1.51 (s, 9 H, Me$_3$), 1.63 (s, br, 1 H, BCH), 1.92 (s, 3 H, =CMe), 1.99 (s, 3 H, =CMe), 2.14 (s, br, 1 H, BCH), 5.39 (s, 1 H, NH), 6.93 (s, 1 H, NH)	247.0 (C=Mo), 178.4 (br, NC), 175.0 (C=O), 172.0 (br, NC), 64.7, 61.2, 60.2 (*C*Me$_3$), 58.1, 57.5 (C=C), 51.3 (*C*Me$_3$), 50.6, 44.3 (br, BCH), 31.5, 30.9, 29.5, 29.4 (C*Me*$_3$), 19.7, 19.3 (=C*Me*)
8b	1.17 (s, 9 H, Me$_3$), 1.35 (s, 9 H, Me$_3$), 1.49 (s, 9 H, Me$_3$), 1.51 (s, 9 H, Me$_3$), 1.92 (s, br, 1 H, BCH), 2.12 (s, 3 H, =CMe), 2.17 (s, 3 H, =CMe), 2.38 (s, br, 1 H, BCH), 5.40 (s, 1 H, NH), 6.59 (s, 1 H, NH)	238.5 [C=W, J(WC) = 59], 176.3 (C=O), 169.8, 167.1 (NC), 60.1, 59.6, 58.6, 58.0 (*C*Me$_3$), 51.4, 51.3 (C=C), 48.2, 41.6 (br, BCH), 31.9, 31.0, 29.7, 29.5 (C*Me*$_3$), 20.1, 19.4 (=C*Me*)
9	1.10 (s, 3 H, Me), 1.53 (s, 36 H, Me$_3$), 3.33 (s, br, 2 H, CH)	154.6 (br, NC), 122.5 [q, br, CF$_3$, J(FC) = 318], 59.8 (*C*Me$_3$), 52.1 (br, CH), 29.8 (C*Me*$_3$), 17.0 (Me)
10[d]	1.39, *1.41 (s, 18 H, Me$_3$), 1.55, *1.59 (s, 9 H, Me$_3$), 1.67, *1.69 (s, 9 H, Me$_3$), 3.02 (s, 3 H, =CMe), 3.20 (s, br, 2 H, BCH), *3.41 (s, 3 H, =CMe), *3.65 (s, br, 2 H, BCH)	194.4, *182.0 (η^2-C=N), *152.3, 150.2 (br, 2 × NC), *146.2, 143.3 (br, NC), 121.2 [q, CF$_3$, J(FC) = 321], *65.4, 64.3 (*C*Me$_3$), 61.1, *60.7 (*C*Me$_3$), 60.0 (2 × *C*Me$_3$), *59.7 (2 × *C*Me$_3$), 52.5, *52.0 (BCH), *30.7, 30.2, 30.1 (C*Me*$_3$), *29.9, 29.6 (2 × C*Me*$_3$), *29.5 (C*Me*$_3$), 19.6, *18.7 (=C*Me*)

[a] Measured at ambient temperatures in CD_2Cl_2. Coupling constants (J) in Hz. [b] Proton resonances for terminal B–H groups occur as broad unresolved peaks in the range δ ca. –2 to +3. [c] Hydrogen-1 decoupled, chemical shifts are positive to high frequency of $SiMe_4$. [d] Peaks marked with an asterisk are assigned to a minor isomer; see text.

Table 3. Boron-11 NMR[a] **Data**

compd	^{11}B/δ
5c	–5.4 (3 B), –8.5 (1 B), –12.4 (2 B), –16.2 (3 B)
6	–2.5 (1 B), –6.9 (2 B), –8.9 (3 B), –10.5 (3 B)
7a	–2.1 (1 B), –5.7 (3 B), –7.4 (1 B), –9.6 (1 B), –12.7 (2 B), –14.6 (1 B)
7b	–2.7 (1 B), –8.4 (3 B), –13.0 (2 B), –18.9 (2 B), –21.4 (1 B)
7c	–4.2 (1 B), –7.2 (1 B), –8.2 (2 B), –14.1 (2 B), –18.4 (2 B), –21.9 (1 B)
8a	–2.5 (1 B), –8.4 (4 B), –10.2 (1 B), –11.6 (1 B), –19.3 (1 B), –20.9 (1 B)
8b	–4.7 (1 B), –8.3 (2 B), –8.6 (2 B), –11.7 (1 B), –12.8 (1 B), –20.0 (1 B), –21.1 (1 B)
9	6.7 (1 B), 5.5 (1 B), –3.3 (2 B), –8.3 (2 B), –12.5 (2 B), –18.4 (1 B)
10[b]	9.6 to –18.0 (9 B)

[a] Hydrogen-1 decoupled, measured at ambient temperatures in CD_2Cl_2. Chemical shifts are positive to high frequency of $BF_3 \cdot Et_2O$ (external). Signals ascribed to more than one boron nucleus may result from overlapping peaks and do not necessarily indicate symmetry equivalence. [b] Peaks are difficult to assign due to existence of two isomers.

8 did not become apparent until after an X-ray diffraction study on **8b** had been carried out.

The molecular structure of **8b** is shown in Figure 1, and selected bond distances and angles are collected in Table 4. The tungsten atom is ligated in the usual pentahapto manner by a *nido*-icosahedral $C_2B_9H_{11}$ fragment [W–C(1) = 2.36(1) Å, W–C(2) = 2.34(1) Å, W–B(3) = 2.40(1) Å, W–B(4) = 2.43(1) Å, W–B(5) = 2.44(1) Å]. The somewhat longer W–B connectivities compared with the W–C bonds are not unusual since the former can be either longer or shorter than the latter in structures of this kind.[2] There are two CNBu^t ligands terminally bound to the metal center [W–C(3) = 1.98(1) Å, W–C(8) = 2.06(1) Å; W–C(3)–N(1) = 178.7(7)°, W–C(8)–N(2) = 178.5(8)°]. The most interesting and unexpected feature of the structure is the presence of the C[N(H)Bu^t]C(Me)C(Me)[C(O)N(H)Bu^t] group. This group is η^3 attached to the tungsten via C(15), C(14), and C(22), but the bonding is best described as that of a vinylcarbene. Thus the bond distance W–C(22) [2.018(7) Å] may be compared with the very similar value [2.05(2) Å] found for the C=W bond in the alkylidene tungsten complex [W{=C(H)C$_6$H$_4$Me-4}I(CO)$_2$(η^5-C$_5$H$_5$)].[3]

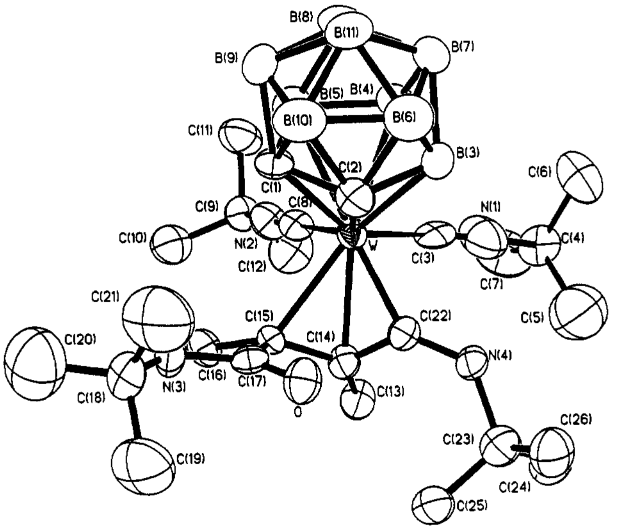

Figure 1. Molecular structure of [W{=C[N(H)Bu^t]C(Me)=C(Me)[C(O)N(H)Bu^t]}(CNBu^t)$_2$(η^5-7,8-C$_2$B$_9$H$_{11}$)] (**8b**) (50% thermal ellipsoids), showing the crystallographic labeling scheme.

Similar data have been obtained for the C=W bonds in other vinylcarbene tungsten complexes: for example, [W{=C(Ph)C(H)=C(H)Me}Br$_2$(CO)$_2$(NC$_5$H$_4$Me-4)] [1.98(2) Å][4a] and [W{=C(Ph)C(Ph)=C(H)C$_6$H$_4$Me-4}I(CO)(η^5-C$_5$H$_5$)] [1.999(7) Å].[4b] The distances W–C(14) [2.308(8) Å] and W–C(15) [2.335(8) Å] in **8b** are typical of those found for η^2-alkene–tungsten complexes.[5] They may be compared with those in [W{=C(Ph)C(H)=C(H)Me}Br$_2$(CO)$_2$(NC$_5$H$_4$Me-4)] [2.38(2), 2.60(2) Å][4a] and in [W{=C(Ph)C(Ph)=C(H)C$_6$H$_4$Me-4}I(CO)(η^5-C$_5$H$_5$)] [2.305(8), 2.293(8) Å].[4b] Notably, the C(13)C(14)C(15)C(16) fragment originates from one of the but-2-yne ligands

---

(3) Howard, J. A. K.; Jeffery, J. C.; Laurie, J. C. V.; Moore, I.; Stone, F. G. A. *Inorg. Chim. Acta* **1985**, *100*, 23.

(4) (a) Mayr, A.; Asaro, M. F.; Glines, T. J. *J. Am. Chem. Soc.* **1987**, *109*, 2215. (b) Garrett, K. E.; Sheridan, J. B.; Pourreau, D. B.; Feng, W. C.; Geoffroy, G. L.; Staley, D. L.; Rheingold, A. L. *J. Am. Chem. Soc.* **1989**, *111*, 8383.

(5) Orpen, A. G.; Brammer, L.; Allen, F. H.; Kennard, O.; Watson, D. G.; Taylor, R. *J. Chem. Soc., Dalton Trans.* **1989**, S1.

Table 4. Selected Internuclear Distances (Å) and Angles (deg) for [W{=C[N(H)Bu^t]C(Me)=C(Me)[C(O)N(H)Bu^t]}(CNBu^t)$_2$(η^5-7,8-$C_2B_9H_{11}$)] (8b), with Estimated Standard Deviations in Parentheses

W–C(3)	1.98(1)	W–C(8)	2.06(1)	W–C(1)	2.36(1)	W–C(2)	2.34(1)
W–B(3)	2.40(1)	W–B(4)	2.43(1)	W–B(5)	2.44(1)	W–C(14)	2.308(8)
W–C(15)	2.335(8)	W–C(22)	2.018(7)	C(1)–C(2)	1.60(1)	C(1)–B(5)	1.67(2)
C(1)–B(9)	1.67(1)	C(1)–B(10)	1.73(2)	C(2)–B(3)	1.72(2)	C(2)–B(6)	1.69(1)
C(2)–B(10)	1.73(2)	B(3)–B(4)	1.79(2)	B(4)–B(5)	1.81(2)	C(3)–N(1)	1.23(2)
N(1)–C(4)	1.43(2)	C(8)–N(2)	1.16(1)	N(2)–C(9)	1.45(1)	C(13)–C(14)	1.47(2)
C(14)–C(15)	1.42(1)	C(14)–C(22)	1.47(1)	C(15)–C(16)	1.54(1)	C(15)–C(17)	1.53(2)
C(17)–O	1.22(1)	C(17)–N(3)	1.35(1)	N(3)–C(18)	1.49(2)	C(22)–N(4)	1.32(1)
N(4)–C(23)	1.49(1)						

C(3)–W–C(8)	80.0(4)	C(3)–W–C(14)	86.8(3)	C(8)–W–C(14)	85.2(3)
C(3)–W–C(15)	120.0(3)	C(8)–W–C(15)	79.9(3)	C(14)–W–C(15)	35.6(3)
C(3)–W–C(22)	79.5(4)	C(8)–W–C(22)	120.9(3)	C(14)–W–C(22)	39.0(3)
C(15)–W–C(22)	64.4(3)	W–C(3)–N(1)	178.7(7)	C(3)–N(1)–C(4)	175(1)
W–C(8)–N(2)	178.5(8)	C(8)–N(2)–C(9)	175(1)	W–C(14)–C(13)	128.9(7)
W–C(14)–C(15)	73.2(4)	C(13)–C(14)–C(15)	127.0(8)	W–C(14)–C(22)	59.7(4)
C(13)–C(14)–C(22)	125.0(8)	C(15)–C(14)–C(22)	107.9(8)	W–C(15)–C(14)	71.2(5)
W–C(15)–C(16)	123.0(6)	C(14)–C(15)–C(16)	117.5(9)	W–C(15)–C(17)	108.7(5)
C(14)–C(15)–C(17)	117.7(7)	C(16)–C(15)–C(17)	112.8(7)	C(15)–C(17)–O	121.7(8)
C(15)–C(17)–N(3)	116.5(8)	O–C(17)–N(3)	122(1)	C(17)–N(3)–C(18)	127.5(8)
W–C(22)–C(14)	81.3(5)	W–C(22)–N(4)	142.0(6)	C(14)–C(22)–N(4)	133.3(7)
C(22)–N(4)–C(23)	132.0(7)				

present in the precursor **5c**. Although the hydrogen atoms bonded to N(3) and N(4) were not located in difference Fourier syntheses, the nonlinearity of the bond angles C(17)–N(3)–C(18) [127.5(8)°] and C(22)–N(4)–C(23) [132.0(7)°] indicates their presence, which was confirmed by the ^{1}H NMR data, as discussed later. Moreover, the presence of the oxygen atom bound to C(17) [C(17)–O = 1.22(1) Å] suggests that this atom, and the two hydrogen atoms, originate from trace amounts of adventitious water.

After establishment of the structure of **8b** by X-ray diffraction, the spectroscopic data for both **8a** and **8b** are readily interpreted. For example, two weak bands observed in the IR spectrum of **8a** (Table 1) at 1622 and 1586 cm^{-1} are due to the NC and CO bonds of the vinylcarbene group, although it is impossible at this stage to assign these peaks to a particular functional group. Similar bands are observed in the IR spectrum of **8b**. In the ^{1}H NMR spectrum of **8a** (Table 2) there are two deshielded resonances at δ 5.39 and 6.93 ppm ascribed to the N(H)-Bu^t protons. The four nonequivalent Bu^t groups give signals at δ 1.16, 1.36, 1.49, and 1.51 ppm. Two broad peaks at δ 1.63 and 2.14 ppm are due to the two cage CH moieties.[6] Two singlets at δ 1.92 and 1.99 ppm are assigned to the two =CMe fragments originating from a but-2-yne molecule. In accordance with its vinylcarbene structure, the ^{13}C{^{1}H} NMR spectrum of **8a** shows a deshielded resonance at δ 247.0 ppm due to the C=Mo group. For **8b** the analogous signal occurs at δ 238.5 ppm [J(WC) = 59 Hz]. These chemical shifts may be compared with those observed in the carbene complex [W{=C(H)NEt$_2$}Cl(CO)$_2$(η^5-C_5H_5)] (δ 236.2 ppm)[7] and those in the vinylcarbene complexes [W{=C(Ph)C(H)=C(H)Me}Br$_2$(CO)$_2$(NC$_5$H$_4$-Me-4)] (δ 240.4 ppm)[4a] and [W{=C(Ph)C(Ph)=C(H)C$_6$H$_4$-Me-4}I(CO)(η^5-C_5H_5)] (δ 269.8 ppm).[4b] The two ligated carbon atoms of the vinyl fragment in **8a** give rise to signals at δ 58.1 and 57.5 ppm. Broad peaks at δ 178.4 and 172.0 ppm are due to the two CNBu^t groups and the resonance at δ 175.0 ppm is assigned to the C=O moiety. The remainder of the spectrum is as expected. The ^{13}C{^{1}H} NMR spectrum of compound **8b** can be interpreted in a similar manner.

Scheme 1. Possible Mechanism for the Formation of the Species 8

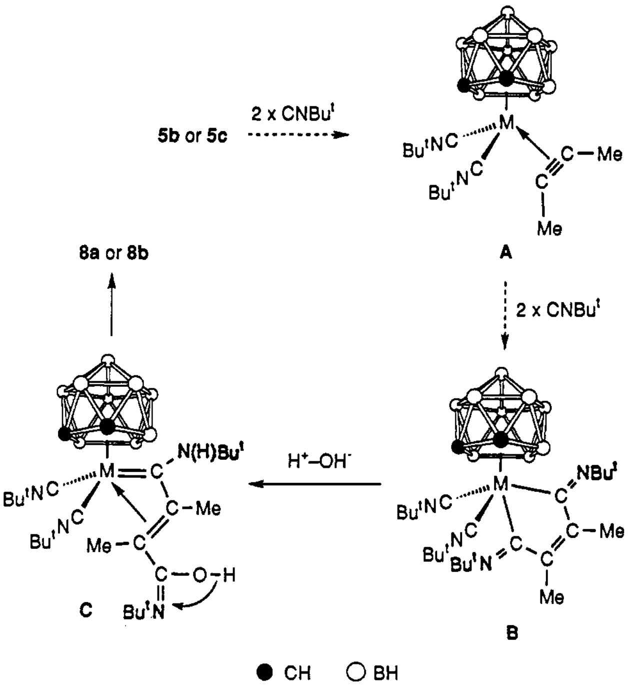

Isolation of the complexes **8** from these reactions was unexpected, and the possible mechanism for their formation is of interest. As shown in Scheme 1 the compounds **5b,c** could react with 2 equiv of CNBu^t to generate the intermediates **A**. The latter could then undergo ligand coupling at the metal centers in the presence of excess of CNBu^t to give species **B**. Coupling of coordinated alkyne and isocyanide groups at metal centers, to yield metallacycles akin to **B**, is well documented.[8] The generated species **B** might then react rapidly with any H_2O present to yield the intermediates **C**. Hydrogen migration from oxygen to nitrogen across the C=N double bond would then afford the observed products **8a,b**. A very similar rearrangement has recently been reported.[9]

---

[6] Brew, S. A.; Stone, F. G. A. *Adv. Organomet. Chem.* **1993**, *35*, 135.

[7] Kreissl, F. R.; Sieber, W. J.; Wolfgruber, M. *J. Organomet. Chem.* **1984**, *270*, C45.

[8] Singleton, E.; Oosthuizen, H. E. *Adv. Organomet. Chem.* **1983**, *22*, 267.

[9] Yeh, W.-Y.; Peng, S.-M.; Liu, L.-K. *Inorg. Chem.* **1993**, *32*, 2965.

Chart 3

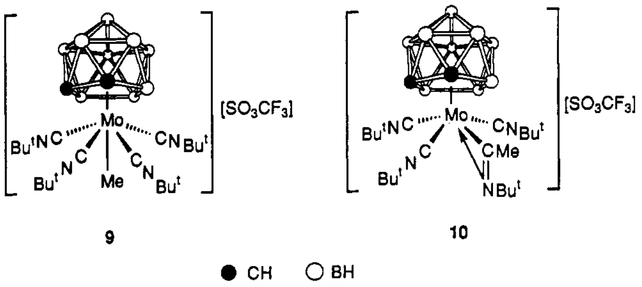

The processes affording the complexes **7** are independent of those giving the compounds **8**. Reactions affording the latter complexes are very much temperature-dependent. A ^{1}H NMR study showed that increasing the concentration of CNBu^t in its reaction with **5c** does not significantly change the ratio of **8b** to **7c** in the product mixture. However, when the reaction between **5c** and excess of CNBu^t was carried out in refluxing CH_2Cl_2 solution, rather than at room temperature, species **8b** was isolated in very low yield, the main product of this reaction being **7c**. Furthermore, treatment of the species **7c** with but-2-yne in wet CH_2Cl_2 does not yield **8b**. Attempts to isolate a complex related to **8b** by adding MeOH to the reaction of **5c** with CNBu^t failed. It is also noteworthy that treatment of a mixture of **5c** and H_2O (1:1 mol ratio) with excess CNBu^t affords **7c** and **8b** in a similar ratio to that obtained when evidently only traces of water are present. Presumably the process affording intermediates **A** or **B** on the pathway to the species **8** is the rate-determining step and is thus independent of the concentration of water. Measurement of the ^{1}H NMR spectra of reaction mixtures did not reveal signals assignable to species of type **A**–**C**. However, this is not surprising since these intermediates could be very reactive and therefore be present in very low concentrations at any given time.

Complexes of type **7** are electron-rich at the metal centers and should therefore react with electrophiles to give cationic carborane–metal species, which are relatively rare. With this in mind, CH_2Cl_2 solutions of **7b** were treated with $HBF_4\cdot Et_2O$ and CF_3SO_3Me, respectively, at room temperature. No stable products were isolated from the protonation reaction, but methylation yielded an orange species formulated as $[MoMe(CNBu^t)_4(\eta^5\text{-}7,8\text{-}C_2B_9H_{11})][SO_3CF_3]$ (**9**) on the basis of NMR studies.

In the ^{1}H NMR spectrum of **9**, there is a relatively shielded singlet at δ 1.10 ppm attributable to three protons. This is typical for methyl groups bound to transition metals. Furthermore, there is only one resonance at δ 1.53 ppm due to the four CNBu^t ligands, indicating these ligands occupy similar environments. Correspondingly, the $^{13}C\{^1H\}$ NMR spectrum of **9** shows peaks at δ 154.6 (NC), 59.8 (*C*Me$_3$), and 29.8 ppm (C*Me*$_3$) for the four equivalent CNBu^t molecules. A signal at δ 17.0 ppm is assigned to the metal-bound methyl group. The broad resonance at δ 52.1 ppm is due to the cage CH nuclei.[6] In addition, the IR and $^{11}B\{^1H\}$ NMR data (Tables 1 and 3) are as expected for the formulation proposed.

Interestingly, when compound **9** (Chart 3) was recrystallized from CH_2Cl_2–petroleum ether, a single-crystal X-ray diffraction study on a selected crystal revealed that the species **9** had undergone rearrangement to afford $[Mo(CNBu^t)_3\{\eta^2\text{-}C(Me){=}NBu^t\}(\eta^5\text{-}7,8\text{-}C_2B_9H_{11})][SO_3CF_3]$ (**10**). The structure of the cation of **10** is shown in Figure 2, and selected bond distances and angles are listed in Table 5.

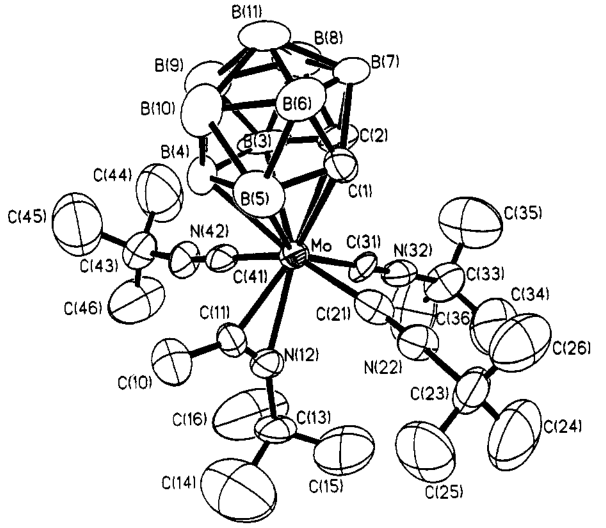

Figure 2. Structure of the cation of $[Mo(CNBu^t)_3\{\eta^2\text{-}C(Me){=}NBu^t\}(\eta^5\text{-}7,8\text{-}C_2B_9H_{11})][SO_3CF_3]$ (**10**) (50% thermal ellipsoids), showing the crystallographic labeling scheme.

The cation consists of a *nido*-7,8-$C_2B_9H_{11}$ cage ligating the metal in the normal pentahapto manner, with three terminally bound CNBu^t groups [Mo–C(21) = 2.14(1) Å, Mo–C(31) = 2.08(1) Å, Mo–C(41) = 2.11(1) Å; Mo–C(21)–N(22) = 174(1)°, Mo–C(31)–N(32) = 179.6(7)°, Mo–C(41)–N(42) = 179.2(9)°] and an η^2-iminoacyl moiety [Mo–C(11) = 2.10(1) Å, Mo–N(12) = 2.14(1) Å]. The bond length C(11)–N(12) [1.19(2) Å] and angles C(10)–C(11)–N(12) [140(1)°] and C(11)–N(12)–C(13) [139(1)°] may be compared with the corresponding values found in $[Mo(CO)_2\{\eta^2\text{-}C(Me){=}NPh\}(\eta^5\text{-}C_5H_5)]$ [C–N = 1.232(6) Å; C–C–N = 134.9(6)°, C–N–C = 138.7(5)°] and are in accord with the η^2-iminoacyl ligand π-bonding.[10]

In order to obtain spectroscopic data for the salt **10**, a CH_2Cl_2 solution of **9** was heated at reflux temperature for 4 days. The NMR studies revealed that the major species in the resulting mixture was complex **10**. This rearrangement of complex **9** was accompanied by some decomposition which gave a trace of an unidentified green species. It is noteworthy that this green impurity was also observed during the crystallization of **9**. The ^{1}H and $^{13}C\{^1H\}$ NMR data (Table 2) of **10** clearly suggest that the complex exists in solution as two isomers, in a ratio of approximately 3:2 based on the integrated intensities in the ^{1}H NMR spectrum. This can be explained if the η^2-iminoacyl group adopts two different orientations, **D** and **E**. **E** can be generated from **D** by rotating the C=N bond of the iminoacyl group 180° along the axis through the molybdenum atom and the midpoint of the C=N bond.

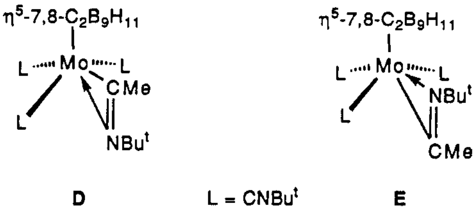

In the solid-state (**D**), there is a mirror plane in the $Mo(CNBu^t)_3\{\eta^2\text{-}C(Me){=}NBu^t\}$ fragment through the Mo, C(10), C(11), N(12), C(13), C(31), and N(32) atoms (Figure

---

[10] Adams, R. D.; Chodosh, D. F. *J. Organomet. Chem.* **1976**, *122*, C11.

Table 5. Selected Internuclear Distances (Å) and Angles (deg) for $[Mo(CNBu^t)_3\{\eta^2\text{-}C(Me){=}NBu^t\}(\eta^5\text{-}7,8\text{-}C_2B_9H_{11})][SO_3CF_3]$ (10), with Estimated Standard Deviations in Parentheses

Mo–C(1)	2.36(1)	Mo–C(2)	2.39(1)	Mo–B(3)	2.38(2)	Mo–B(4)	2.36(2)
Mo–B(5)	2.39(2)	Mo–C(11)	2.10(1)	Mo–N(12)	2.14(1)	Mo–C(21)	2.14(1)
Mo–C(31)	2.08(1)	Mo–C(41)	2.11(1)	C(1)–C(2)	1.56(2)	C(1)–B(5)	1.69(2)
C(1)–B(6)	1.70(2)	C(1)–B(7)	1.74(2)	C(2)–B(3)	1.59(2)	C(2)–B(7)	1.75(2)
C(2)–B(8)	1.69(2)	B(3)–B(4)	1.89(2)	B(4)–B(5)	1.82(2)	C(10)–C(11)	1.46(2)
C(11)–N(12)	1.19(2)	N(12)–C(13)	1.51(2)	C(21)–N(22)	1.16(1)	N(22)–C(23)	1.46(2)
C(31)–N(32)	1.17(2)	N(32)–C(33)	1.48(2)	C(41)–N(42)	1.16(1)	N(42)–C(43)	1.37(2)

C(1)–Mo–C(2)	38.2(4)	C(2)–Mo–B(3)	38.8(4)	B(3)–Mo–B(4)	46.9(6)
C(1)–Mo–B(5)	41.6(5)	B(4)–Mo–B(5)	45.2(5)	C(11)–Mo–N(12)	32.5(4)
C(11)–Mo–C(21)	81.2(4)	N(12)–Mo–C(21)	76.8(4)	C(11)–Mo–C(31)	122.7(5)
N(12)–Mo–C(31)	90.3(4)	C(21)–Mo–C(31)	85.8(4)	C(11)–Mo–C(41)	81.3(4)
N(12)–Mo–C(41)	75.9(4)	C(21)–Mo–C(41)	151.0(5)	C(31)–Mo–C(41)	84.4(4)
Mo–C(1)–C(2)	71.8(6)	Mo–C(1)–B(5)	69.9(8)	C(2)–C(1)–B(5)	115.4(9)
Mo–C(2)–C(1)	69.9(6)	Mo–C(2)–B(3)	70.1(7)	C(1)–C(2)–B(3)	115(1)
Mo–B(3)–C(2)	71.1(7)	Mo–B(3)–B(4)	66.0(7)	C(2)–B(3)–B(4)	104(1)
Mo–B(4)–B(3)	67.0(7)	Mo–B(4)–B(5)	68.3(8)	B(3)–B(4)–B(5)	104.8(9)
Mo–B(5)–C(1)	68.4(8)	Mo–B(5)–B(4)	66.6(8)	C(1)–B(5)–B(4)	101(1)
Mo–C(11)–C(10)	144(1)	Mo–C(11)–N(12)	75.7(7)	C(10)–C(11)–N(12)	140(1)
Mo–N(12)–C(11)	71.8(7)	Mo–N(12)–C(13)	149.1(8)	C(11)–N(12)–C(13)	139(1)
N(12)–C(13)–C(14)	114(2)	N(12)–C(13)–C(15)	112(1)	N(12)–C(13)–C(16)	108(1)
Mo–C(21)–N(22)	174(1)	C(21)–N(22)–C(23)	176(1)	N(22)–C(23)–C(24)	109(1)
N(22)–C(23)–C(25)	107(1)	N(22)–C(23)–C(26)	110(1)	Mo–C(31)–N(32)	179.6(7)
C(31)–N(32)–C(33)	178(1)	N(32)–C(33)–C(34)	107(1)	N(32)–C(33)–C(35)	107(2)
N(32)–C(33)–C(36)	109(1)	Mo–C(41)–N(42)	179.2(9)	C(41)–N(42)–C(43)	170(1)
N(42)–C(43)–C(44)	109(1)	N(42)–C(43)–C(45)	110(1)	N(42)–C(43)–C(46)	116(1)

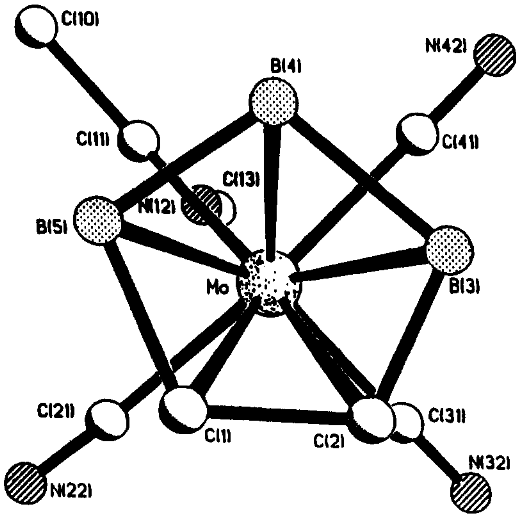

Figure 3. Simplified view of ligand arrangement in the solid state of complex 10.

3), and this is evident from the NMR data. Thus, in the ^1H NMR spectrum, a singlet at δ 1.39 ppm is attributable to the two equivalent *transoid* $CNBu^t$ groups of the major isomer. For the minor isomer, the resonance due to these protons occurs at δ 1.41 ppm. Because there is a mirror plane and with the carborane cage rotating, the two cage CH groups are equivalent, thus giving rise to a single broad resonance at δ 3.20 ppm for the major isomer and a signal at δ 3.65 ppm for the minor isomer. The CMe protons of the η^2-iminoacyl groups resonate at δ 3.02 (major isomer) and 3.41 ppm (minor isomer). The remainder of the ^1H NMR data is as expected. The $^{13}C\{^1H\}$ NMR measurements also support the presence of two isomers. Thus two relatively deshielded resonances at δ 194.4 and 182.0 ppm are assigned to the η^2-C=N nuclei of the major and minor isomers, respectively, on the basis of their relative intensities. These values are similar to those observed in the spectra of the iminoacyl complexes $[Mo(CO)_2\{\eta^2\text{-}C(Et){=}NEt\}(\eta^5\text{-}C_5H_5)]$ (δ 197.8 ppm)[11a] and $[W(CO)_2\{\eta^2\text{-}C(Me){=}NEt\}(\eta^5\text{-}C_5Me_5)]$ (δ 194.7 ppm).[11b] The C*Me* fragments give signals at δ 19.6 (major isomer) and 18.7 ppm (minor isomer). The equivalent *transoid* $CNBu^t$ groups are revealed by resonances at δ 150.2, 60.0, and 29.6 ppm for the major isomer and at δ 152.3, 59.7, and 29.9 ppm for the minor isomer.

The rearrangement process 9 into 10, i.e. formally insertion of the isocyanide ligand into the metal–alkyl bond to give an iminoacyl moiety, has ample precedent.[8,11] For example, η^2-iminoacyl complexes $[W(CO)_2\{\eta^2\text{-}C(R){=}NEt\}(\eta^5\text{-}C_5Me_5)]$ (R = Me, Et) are isolated from the reaction mixture generated by refluxing the alkyl–metal species $[WR(CO)_2(CNEt)(\eta^5\text{-}C_5Me_5)]$ (R = Me, Et) in toluene. These products also form together with the 1-azaallyl compounds $[W(CO)_2\{\eta^3\text{-}CH(R')CHNEt\}(\eta^5\text{-}C_5Me_5)]$ (R′ = H, Me).[11] The above mentioned unidentified green species could thus be a 1-azaallyl–carborane complex of molybdenum.

Conclusions

The metallacarborane complexes described in this paper further illustrate the synthesis of new species obtainable from (alkyne)(carborane)molybdenum and -tungsten compounds such as 5. As far as we are aware, the products 8, containing the vinylcarbene ligand $:C\{N(H)Bu^t\}C(Me){=}C(Me)\{C(O)N(H)Bu^t\}$, are structurally without precedent. Also the complexes 9 and 10 are unusual in that they are cationic species containing a *nido*-carborane cage. Further studies on compounds of this type are underway.

Experimental Section

General Considerations. All reactions were carried out under an atmosphere of nitrogen (99+% dry), using Schlenk tube techniques. Solvents were distilled under nitrogen from appropriate drying agents before use. Petroleum ether refers to that fraction of bp 40–60 °C. Chromatography columns (ca. 15 cm in length and 2 cm in diameter) were packed with silica gel (Aldrich, 70–230 mesh) or with alumina (Aldrich, Brockmann activity III). The NMR spectra (Tables 2 and 3) were recorded at the following frequencies: 360.1 MHz for ^1H, 90.6 MHz for

---

[11] (a) Filippou, A. C.; Fischer, E. O.; Grunleitner, W. *J. Organomet. Chem.* **1990**, *386*, 333. (b) Filippou, A. C.; Grunleitner, W.; Kiprof, P. *J. Organomet. Chem.* **1991**, *410*, 175 and references cited therein.

^{13}C, and 115.5 MHz for ^{11}B. The reagents **5a,b** were prepared as described previously.[1a] Tetrafluoroboric acid was an 85% solution of $HBF_4{\cdot}Et_2O$ in Et_2O, as supplied by Aldrich Chemical Co.

Synthesis of the Salt $[N(PPh_3)_2][W(CO)_2(\eta^3\text{-}C_3H_5)(\eta^5\text{-}7,8\text{-}C_2B_9H_{11})]$. A thf (30 mL) solution of $[WBr(CO)_2(NCMe)_2(\eta^3\text{-}C_3H_5)]$[12] (1.40 g, 3.16 mmol) at room temperature was treated with a thf (20 mL) solution of $Na_2[7,8\text{-}C_2B_9H_{11}]$. The latter was generated from $[NHMe_3][7,8\text{-}C_2B_9H_{12}]$ (0.50 g, 2.58 mmol) and NaH (60% dispersion in mineral oil, 0.50 g, 12.50 mmol, washed with 2 × 10 mL of thf) at reflux temperature for 12 h. After stirring of the mixture for 0.5 h, $[N(PPh_3)_2]Cl$ (1.65 g, 2.87 mmol) was added and stirring was continued for 0.5 h, after which time solvent was removed in vacuo. The residue was extracted with CH_2Cl_2 (10 mL), and the extract was chromatographed on silica gel at −20 °C. Elution with CH_2Cl_2–petroleum ether (4:1) gave a yellow eluate. After solvent was removed in vacuo, the crude product was crystallized from CH_2Cl_2–petroleum ether (30 mL, 1:5) and dried in vacuo to give yellow *microcrystals* of $[N(PPh_3)_2][W(CO)_2(\eta^3\text{-}C_3H_5)(\eta^5\text{-}7,8\text{-}C_2B_9H_{11})]$ (1.61 g, 65%). Anal. Found: C, 50.9; H, 4.9; N, 1.9. Calcd for $C_{43}H_{46}B_9NO_2P_2W{\cdot}CH_2Cl_2$: C, 51.0; H, 4.7; N, 1.4. ν_{max}(CO) is at 1919 vs and 1826 vs cm^{-1} in CH_2Cl_2. NMR (in CD_2Cl_2) (J values in Hz): ^{1}H, δ 1.29 [d of t, 2 H, H_{anti}, $J(H_{anti}H_{cent})$ = 10, $J(H_{anti}H_{syn})$ = 1], 2.04 (s, br, 2 H, BCH), 2.75 [t of t, 1 H, H_{cent}, J(HH) = 10, 7], 2.93 [d of t, 2 H, H_{syn}, $J(H_{syn}H_{cent})$ = 7, $J(H_{syn}H_{anti})$ = 1], 7.44–7.64 ppm (m, 30 H, Ph); ^{13}C{^{1}H}, δ 231.6 [CO, J(WC) = 167], 134.1–126.8 (Ph), 71.9 (CH of C_3H_5), 40.3 (br, BCH), 37.3 ppm [CH_2, J(WC) = 8]; ^{11}B{^{1}H}, δ −5.9 (1 B), −7.2 (3 B), −11.3 (1 B), −14.7 (2 B), −19.6 ppm (2 B).

Preparation of the Complex $[W(CO)(\eta^2\text{-}MeC_2Me)_2(\eta^5\text{-}7,8\text{-}C_2B_9H_{11})]$ (5c). A CH_2Cl_2 (10 mL) solution of $[N(PPh_3)_2][W(CO)_2(\eta^3\text{-}C_3H_5)(\eta^5\text{-}7,8\text{-}C_2B_9H_{11})]$ (0.50 g, 0.53 mmol) and but-2-yne (0.50 mL, 6.39 mmol) was treated with $HBF_4{\cdot}Et_2O$ (0.10 mL, 0.58 mmol) at −78 °C, and the mixture was warmed to room temperature and stirred for 2 h. Solvent was removed in vacuo, the residue was extracted with CH_2Cl_2–petroleum ether (1:1, 10 mL), and the solution was filtered through a short silica gel column (ca. 5 cm in length and 2 cm in diameter) at −20 °C. Elution with the same solvent mixture gave a pink eluate from which the solvent was removed in vacuo and the product was washed with petroleum ether (3 × 2 mL) to remove a trace of a purple impurity. Drying of the product in vacuo gave pale yellow *microcrystals* of $[W(CO)(\eta^2\text{-}MeC_2Me)_2(\eta^5\text{-}7,8\text{-}C_2B_9H_{11})]$ (**5c**) (0.15 g).

Reactions of the Complexes $[M(CO)(\eta^2\text{-}MeC_2Me)_2(\eta^5\text{-}7,8\text{-}R'_2\text{-}7,8\text{-}C_2B_9H_9)]$ (5) with CNBu^t. (i) A mixture of **5a** (0.20 g, 0.51 mmol) and CNBu^t (0.24 mL, 2.13 mmol) was stirred in CH_2Cl_2 (10 mL) overnight, during which time a color change from yellow to orange was observed. Solvent was removed in vacuo, the residue was dissolved in CH_2Cl_2 (2 mL), and the solution was chromatographed on alumina. Elution using CH_2Cl_2 yielded initially a yellow band. Solvent was removed in vacuo, and the residue crystallized from CH_2Cl_2–petroleum ether (1:4, 10 mL) to give yellow *microcrystals* of $[Mo(CO)(CNBu^t)_3(\eta^5\text{-}7,8\text{-}Me_2\text{-}7,8\text{-}C_2B_9H_9)]$ (**6**) (0.08 g). Further elution of the column with CH_2Cl_2 gave a second yellow eluate. Solvent was removed in vacuo, and crystallization of the residue as above afforded yellow *microcrystals* of $[Mo(CNBu^t)_4(\eta^5\text{-}7,8\text{-}Me_2\text{-}7,8\text{-}C_2B_9H_9)]$ (**7a**) (0.13 g).

(ii) A mixture of **5b** (0.20 g, 0.55 mmol) and CNBu^t (0.25 mL, 2.21 mmol) was stirred in CH_2Cl_2 (10 mL) for ca. 15 h, during which time a color change from yellow to orange was observed. Solvent was removed in vacuo, the residue was extracted with CH_2Cl_2–petroleum ether (1:1, 10 mL), and the extract was chromatographed on alumina. Elution with the same solvent mixture yielded initially a yellow fraction. Solvent was removed in vacuo, and the residue crystallized from CH_2Cl_2–petroleum ether (1:4, 10 mL) to give yellow *microcrystals* of $[Mo(CNBu^t)_4(\eta^5\text{-}7,8\text{-}C_2B_9H_{11})]$ (**7b**) (0.19 g). Further elution with neat CH_2Cl_2 gave an orange-red eluate. Solvent was removed in vacuo, and crystallization of the residue, as described above for **7b**, afforded orange-red *microcrystals* of $[Mo\{{=}C[N(H)Bu^t]C(Me){=}C(Me)[C(O)N(H)Bu^t]\}(CNBu^t)_2(\eta^5\text{-}7,8\text{-}C_2B_9H_{11})]$ (**8a**) (0.04 g).

(iii) Similarly, a mixture of **5c** (0.10 g, 0.22 mmol) and CNBu^t (0.24 mL, 2.13 mmol) was stirred in CH_2Cl_2 (20 mL) for ca. 12 h. Following the same purification process as above, yellow *microcrystals* of $[W(CNBu^t)_4(\eta^5\text{-}7,8\text{-}C_2B_9H_{11})]$ (**7c**) (0.05 g) and orange-red *microcrystals* of $[W\{{=}C[N(H)Bu^t]C(Me){=}C(Me)[C(O)N(H)Bu^t]\}(CNBu^t)_2(\eta^5\text{-}7,8\text{-}C_2B_9H_{11})]$ (**8b**) (0.06 g) were isolated.

Methylation of the Compound $[Mo(CNBu^t)_4(\eta^5\text{-}7,8\text{-}C_2B_9H_{11})]$ (7b) with CF_3SO_3Me. To a CH_2Cl_2 (10 mL) solution of **7b** (0.10 g, 0.18 mmol) was added CF_3SO_3Me (0.02 mL, 0.18 mmol), and the mixture was stirred for 14 h. Solvent was reduced to ca. 2 mL in vacuo, and petroleum ether (10 mL) was slowly added with rapid stirring. The supernatent liquid was decanted to leave orange *microcrystals* of $[MoMe(CNBu^t)_4(\eta^5\text{-}7,8\text{-}C_2B_9H_{11})][SO_3CF_3]$ (**9**) (0.09 g).

Rearrangement of the Complex $[MoMe(CNBu^t)_4(\eta^5\text{-}7,8\text{-}C_2B_9H_{11})][SO_3CF_3]$ (9). A CH_2Cl_2 (20 mL) solution of the salt **9** (0.10 g, 0.14 mmol) was heated at reflux temperature for 4 days. Solvent was removed in vacuo, and the residue was crystallized from CH_2Cl_2–petroleum ether (1:4, 10 mL) to give $[Mo(CNBu^t)_3\{\eta^2\text{-}C(Me){=}NBu^t\}(\eta^5\text{-}7,8\text{-}C_2B_9H_{11})][SO_3CF_3]$ (**10**) (0.06 g), contaminated with an unidentified green species.

Crystal Structure Determinations and Refinements. The crystal data and experimental parameters for compounds **8b** and **10** are given in Table 6. Orange crystals of **8b** were grown from CH_2Cl_2 layered with petroleum ether. Crystals of **10** were obtained from a CH_2Cl_2–petroleum ether solution of **9** by slow diffusion in an attempt to grow crystals of **9**. The cell dimensions were determined from the setting angle values of 25 accurately centered reflections for both **8b** and **10**. Two (**8b**) or three (**10**) check reflections were measured every 2 h. The crystal of **8b**

Table 6. Data for Crystal Structure Analysis of Compounds 8b and 10[a]

	8b	**10**
cryst dimens/mm	0.08 × 0.16 × 0.46	0.10 × 0.25 × 0.59
molecular formula	$C_{26}H_{55}B_9N_4OW$	$C_{24}H_{50}B_9F_3MoN_4O_3S$
M_r	720.9	725.0
cryst color, shape	orange rectangles	orange rectangular plates
cryst system	triclinic	monoclinic
space group (No.)	$P\bar{1}$ (2)	$C2/c$ (15)
a/Å	10.913(2)	41.569(4)
b/Å	11.992(2)	9.465(2)
c/Å	14.852(2)	20.381(2)
α/deg	73.12(1)	
β/deg	82.478(13)	105.616(7)
γ/deg	74.14(2)	
V/Å^3	1786.3(5)	7697(2)
Z	2	8
d_{calcd}/g cm^{-3}	1.346	1.251
$F(000)$/e	732	3008
μ(Mo Kα)/cm^{-1}	33.32	4.27
scan speed/deg min^{-1}	0.46–5.17	0.48–3.44
scan range (ω, deg)	1.20 + 0.344 tan θ	1.25 + 0.34 tan θ
2θ range/deg	3.0–40.0	3.0–40.0
no. of unique data	3302	3579
no. of obsd data used	3098	2770
criterion for obsd data, n in $F \geq n\sigma(F)$	4	6
R (R')[b]	0.034 (0.041)	0.085 (0.095)
resid density (max, min/e Å^{-3})	0.84, −0.94	1.35, −0.63

[a] Data collected at 292 K on an Enraf-Nonius CAD4-F automated diffractometer operating in the ω–2θ scan mode; graphite-monochromated Mo Kα X-radiation, $\bar{\lambda}$ = 0.710 73 Å. Refinements were by blocked full-matrix least-squares on F with a weighting scheme of the form $w^{-1} = [\sigma^2(F_o) + g|F_o|^2]$ with g = 0.0030 for **8b** and 0.0026 for **10**; $\sigma^2(F_o)$ is the variance in F_o due to counting statistics: g was chosen so as to minimize variation in $\sum w(|F_o|-|F_c|)^2$ with $|F_o|$. [b] $R = \sum||F_o|-|F_c||/\sum|F_o|$, $R' = \sum w^{1/2}||F_o| - |F_c||/\sum w^{1/2}|F_o|$.

---

[12] Hayter, R. G. *J. Orgnomet. Chem.* **1968**, *13*, P1.

Table 7. Atomic Coordinates ($\times 10^4$) and Equivalent Isotropic Displacement Parameters ($Å^2 \times 10^3$) for 8b

atom	*x*	*y*	*z*	*U*(eq)[a]
W	1215(1)	2844(1)	2443(1)	32(1)
C(1)	−110(8)	3225(8)	1199(7)	48(1)
C(2)	−222(9)	2013(8)	1980(7)	47(1)
B(3)	−746(10)	2302(10)	3056(8)	51(1)
B(4)	−941(10)	3890(10)	2839(8)	51(1)
B(5)	−495(10)	4444(10)	1607(8)	52(1)
B(6)	−1771(10)	2099(10)	2351(9)	53(1)
B(7)	−2291(10)	3281(10)	2842(8)	47(1)
B(8)	−2129(10)	4617(10)	1986(9)	59(1)
B(9)	−1538(10)	4155(11)	916(8)	61(1)
B(10)	−1380(11)	2638(11)	1157(9)	65(1)
B(11)	−2617(10)	3469(10)	1701(9)	58(1)
C(3)	1400(8)	2916(8)	3732(7)	44(1)
N(1)	1541(9)	2950(10)	4529(7)	85(1)
C(4)	1760(10)	2877(9)	5473(6)	57(1)
C(5)	2473(14)	1635(12)	5907(10)	131(1)
C(6)	488(11)	3381(11)	5914(9)	94(1)
C(7)	2601(12)	3715(11)	5397(10)	102(1)
C(8)	2077(8)	4252(8)	2130(6)	33(1)
N(2)	2559(7)	5043(7)	1976(6)	49(1)
C(9)	3117(9)	6049(8)	1864(7)	48(1)
C(10)	3956(10)	6184(9)	949(8)	66(1)
C(11)	1987(10)	7168(9)	1829(8)	71(1)
C(12)	3905(11)	5758(10)	2715(9)	80(1)
C(13)	4355(8)	1698(9)	2965(7)	48(1)
C(14)	3269(8)	1638(8)	2510(6)	35(1)
C(15)	3011(8)	2113(7)	1543(6)	36(1)
C(16)	3848(8)	2914(8)	914(6)	41(1)
C(17)	2678(8)	1291(7)	1044(6)	32(1)
O	2380(6)	360(5)	1485(4)	46(1)
N(3)	2734(8)	1644(7)	93(5)	52(1)
C(18)	2519(9)	993(8)	−561(6)	43(1)
C(19)	3408(12)	−223(10)	−387(9)	93(1)
C(20)	2760(14)	1704(12)	−1521(9)	121(1)
C(21)	1185(12)	831(12)	−404(10)	113(1)
C(22)	2199(8)	1141(7)	3006(6)	37(1)
N(4)	2129(7)	169(6)	3695(5)	36(1)
C(23)	3061(9)	−1014(8)	4017(7)	51(1)
C(24)	3607(9)	−1038(9)	4919(7)	53(1)
C(25)	4138(9)	−1241(8)	3281(7)	51(1)
C(26)	2300(10)	−1948(9)	4223(8)	62(1)

[a] Equivalent isotropic *U* defined as one-third of the trace of the orthogonalized U_{ij} tensor.

showed no significant variation over the period of data collection (<2.3%). Slow decay of **10** (0.0476%/h) necessitated use of the program DECAY.[13] After removal of check intensity data, averaging of duplicate and equivalent measurements was performed, the systematic absences were deleted, and the remaining data were corrected for Lorentz, polarization, and X-ray absorption effects, the latter by an empirical method based upon azimuthal scan data.[13]

Table 8. Atomic Coordinates ($\times 10^4$) and Equivalent Isotropic Displacement Parameters ($Å^2 \times 10^3$) for 10

atom	*x*	*y*	*z*	*U*(eq)[a]
Mo	4019(1)	1131(1)	4107(1)	34(1)
C(1)	4087(3)	1747(12)	3028(6)	47(3)
C(2)	4030(3)	3130(12)	3396(6)	48(3)
B(3)	4285(4)	3359(16)	4122(8)	66(3)
B(4)	4577(3)	1804(17)	4218(7)	52(3)
B(5)	4410(4)	738(20)	3457(8)	70(3)
B(6)	4428(4)	1931(19)	2724(9)	69(3)
B(7)	4184(4)	3321(17)	2683(8)	56(3)
B(8)	4325(5)	4376(19)	3413(7)	75(3)
B(9)	4687(5)	3499(19)	3946(9)	76(3)
B(10)	4764(4)	1913(23)	3543(9)	87(3)
B(11)	4604(4)	3519(18)	3043(8)	71(3)
C(10)	4469(3)	−1823(15)	4685(8)	74(3)
C(11)	4195(3)	−809(12)	4566(6)	45(3)
N(12)	3941(2)	−618(10)	4715(4)	46(2)
C(13)	3737(4)	−1304(13)	5138(6)	67(3)
C(14)	3846(6)	−2754(19)	5363(14)	186(3)
C(15)	3400(5)	−1463(25)	4767(11)	172(3)
C(16)	3751(6)	−319(25)	5781(11)	180(3)
C(21)	3708(3)	−255(11)	3376(5)	48(3)
N(22)	3533(3)	−1062(10)	3026(5)	50(2)
C(23)	3334(3)	−2150(15)	2594(7)	69(3)
C(24)	2996(5)	−2250(23)	2739(11)	149(3)
C(25)	3492(6)	−3553(16)	2838(10)	126(3)
C(26)	3319(5)	−1874(19)	1870(9)	106(3)
C(31)	3575(3)	2049(12)	4184(6)	43(3)
N(32)	3326(2)	2558(10)	4224(5)	49(3)
C(33)	3001(3)	3161(14)	4256(7)	64(3)
C(34)	2744(5)	2186(22)	3909(12)	154(3)
C(35)	2965(5)	4455(18)	3898(11)	145(3)
C(36)	2990(5)	3211(25)	4934(10)	148(3)
C(41)	4211(3)	1842(12)	5121(5)	41(3)
N(42)	4320(2)	2225(10)	5678(4)	48(2)
C(43)	4480(3)	2838(15)	6288(7)	70(3)
C(44)	4445(6)	4469(20)	6222(11)	160(3)
C(45)	4850(5)	2748(24)	6404(12)	156(3)
C(46)	4349(5)	2495(21)	6857(8)	129(3)
C	2774(5)	2781(23)	1200(9)	183(3)
F(1)	2901(10)	3480(31)	825(18)	219(3)
F(2)	2803(6)	1732(23)	778(10)	292(3)
F(3)	2672(7)	1974(32)	1778(15)	176(3)
F(4)	2589(6)	3772(20)	1384(11)	280(3)
S(1)	3190(3)	3044(11)	1742(6)	105(3)
S(2)	3056(2)	2240(8)	1989(4)	73(2)
O(1)	3340(5)	1671(19)	1770(10)	178(3)
O(2)	3253(9)	4178(28)	1333(15)	165(3)
O(3)	3179(6)	3301(18)	2495(9)	224(3)
O(4)	2828(6)	1299(24)	2180(15)	134(3)

[a] Equivalent isotropic *U* defined as one-third of the trace of the orthogonalized U_{ij} tensor.

The structure of **8b** was solved by conventional heavy-atom methods, and that of **10** was solved by direct methods. Successive Fourier difference syntheses were used to locate all the non-hydrogen atoms which were refined anisotropically. All hydrogen atoms were included at geometrically calculated positions (C–H = 0.96 Å, B–H = 1.10 Å, N–H = 0.96 Å) using a riding model with fixed isotropic thermal parameters ($U_{iso} = 80 \times 10^{-3}$, 60×10^{-3}, and 80×10^{-3} Å^2, respectively). The SO_3CF_3 anion of the salt **10** is disordered such that the sulfur atom, one of the oxygen atoms, and one of the fluorine atoms occupy one of two sites (50% occupancy) related by reflection through the plane defined by the atoms C, F(2), F(4), O(1), and O(3). Calculations were performed using the SHELXTL-PC package of programs.[13] Atomic scattering factors were taken from ref 14. Final atomic positional parameters for the non-hydrogen atoms are given in Tables 7 (for **8b**) and 8 (for **10**).

Acknowledgment. We thank the Robert A. Welch Foundation for support (Grants AA-1201 and 0668).

Supplementary Material Available: Complete tables of bond lengths and bond angles, anisotropic thermal parameters, and hydrogen atom parameters for **8b** and **10** (18 pages). Ordering information is given on any current masthead page.

OM930642D

---

(13) Siemens: SHELXTL-PC Siemens X-ray Instruments, Madison, WI, 1989.

(14) *International Tables for X-ray Crystallography*; Kynoch Press: Birmingham, U.K., 1974; Vol. 4.